Indian J. Met. Hydrol. Geophys., (1978), **29**, 1 & 2, 314-326

551.553.21 : 551.509.313 : 551.513.1

*Simulation of the global monsoon sequence by a simple ocean-atmosphere interaction model**

PETER J. WEBSTER and KA MING W. LAU

Department of Atmospheric Sciences, University of Washington, Seattle, Washington

ABSTRACT. A simple model is utilized to study the annual monsoon sequence of an atmosphere-ocean system constructed to approximate the gross features of the continent-ocean distribution of the earth. The general three-dimensional structure of the system is simplified by division into a number of domains, so chosen as to isolate regions of similar character or similar lower boundary conditions. The governing primitive equations are averaged in longitude between the limits of each domain and neighbouring domains interact *via* east-west interdomain fluxes of heat and momentum. From this process, coupled sets of two-dimensional primitive equations evolve in latitude-height plane. The oceans are represented as simple advective mixed layers in which the vertical structure is represented by two layers and advection forced by the latitudinal density variation.

To accomplish the horizontal coupling of adjacent domains, a parameterization is developed based on the theory of slowly-varying or quasi-stationary modes. The character of the parameterization is such as to reduce to a quasi-geostrophic nature in mid-latitudes and to a longitude-height plane confinement at low latitudes, the latter consistent with an east-west Walkertype solution. Coupling between the ocean and the atmosphere is accomplished by wind stress and lower boundary heating.

Results are presented for a four-domain version of the model in which solar heating is allowed to follow an annual cycle. The effect of the vastly different time scales introduced into the model by the land and ocean regions is most marked in providing a diversity of response between hemispheres at different seasons and between land and ocean domains. The most interesting features are the rapid equinoctial transitions and the development of a strong easterly jet stream in the early northern hemisphere summer and its rapid decay in early autumn; features which the oceanic southern hemisphere does not reproduce.

1. Introduction

During the past two decades or so, detailed and careful analyses of various data sets have succeeded in identifying pertinent features and providing important and informative descriptions of both mean and transient features of the Asian monsoon system. Such analyses have emerged from the International Indian Ocean Expedition (summarized by Ramage and Raman 1972, in atlas form and in more general terms by Ramage 1971) and from composite data sets compiled from a number of sources including satellite imagery (*e.g.*, Sadler 1969, 1975 and Sadler and Harris 1970). Emerging from these studies is a picture of a fairly reproducible slowly varying seasonal structure with a variety of transients of various space and time scales superimposed upon it. Such transients may or may not reappear from year to year or exhibit the same regularity. Apparent then is that there is not the dominance of one physical process beyond the annual variation of solar heating and the relative position of land and oceans, but possibly a complex interplay of many competing processes.

In the last ten years numerical and theoretical modelling has succeeded in reproducing some of

*Contribution Number 404, University of Washington, Department of Atmospheric Sciences, AK-40, Seattle, Washington.

the gross climatological features of the Asian monsoon system if not the details of its variability (*e.g.*, breaks and depression development) and precise field location (*e.g.*, precipitation maxima). Most of these gains may be attributed to groups engaged in the development of large-scale and highly sophisticated general circulation models (*e.g.*, as used in monsoon studies by Washington and Daggapaty 1975, Hahn and Manabe 1975). Some progress has been made in using such models to suggest physical processes involved in the variability of the system (*e.g.*, Shukla 1975).

Most numerical studies emphasize variations about July or January mean conditions or the simulation of a mean climatology itself, with the exception of a few studies, in particular that of Hahn and Manabe (1975), the transient monsoon system has received little attention. This is not surprising as the study of what effectively is a global monsoon cycle requires consideration of models which possess an interactive and dynamic ocean system. The necessity of such an inclusion is prompted by the mutual importance of oceans and atmospheres over a wide range of space and time scales. For example, consideration of an interactive ocean is necessary in order to duplicate a correctly phased annual cycle. This is obvious from the observation that in the summer hemisphere the maximum sea surface temperature at mid-latitudes occurs many weeks after the summer solstice, whereas maximum temperatures over land occur only shortly after the solstice.

The development of an interactive model is an extremely difficult process and only recently accomplished in the general circulation model scale by Bryan *et al.* (1975) and Manabe *et al.* (1975). Whereas the coupled model described in these two papers has succeeded in underlining the importance treating the *total* system as a necessary prerequisite in providing an adequate description of even a mean climatic state, the complexity and size of such a model places severe logistical constraints on experimentation.

With the logistical difficulties of the general circulation model in mind and deciding upon a philosophy of attempting to use the simplest possible model which will contain many of the important interactive processes involved in an annual cycle, we will use the simple phenomenological model developed by Webster and Lau (1976). The basic aim is to simulate an annual monsoon sequence of an extremely simple earth atmosphere-ocean system.

The basic structure of the model is defined by dividing the atmosphere and ocean into a series of truncated domains. The domain is only constrained in *longitude* and a domain is chosen to isolate regions of similar character or similar lower boundary condition. The basic equations are written for each domain and averaged in longitude, but only to the limits of each domain. What emerges are systems of differential equations for *each* domain which are functions of *time*, *height* and *latitude*. The basic domain structure to which we apply our system is shown in Fig. 2 which shows a 4-domain structure. The first atmospheric domain (A1) overlays the northern hemisphere continent and the truncated ocean to the south (01). The second atmospheric domain overlays the pole-to-pole ocean (02). Oceans 01 and 02 are explicitly coupled to atmospheres A1 and A2, respectively. Atmospheres A1 and A2 are connected by inter-domain fluxes of heat and momentum and by interaction terms. Solution of the systems of equations will provide latitude-height-time structure of each domain; A1, A2, 01 and 02.

In the next section we will develop the theoretical basis for the model. In section 3 we will present the results of a simple annual cycle experiment. We conclude with a critical evaluation of the model and its usefulness and a discussion of future work.

2. The Basic model

Details of the atmospheric model may be found in Webster and Lau (1976) and of the ocean model in Lau (1976). In this paper we will present only the basic formulation of both parts of the domain averaged model.

(a) *The atmosphere*

The primitive equations of motion in spherical coordinates may be written in the following flux form :

$$u_t + g(u) = -\frac{1}{a\cos\phi}\psi_\lambda + v\left(f + \frac{\tan\phi}{a}u\right) + F_1$$

$$v_t + g(v) = -\frac{1}{a}\psi_\phi - u\left(f + \frac{\tan\phi}{a}u\right) + F_2$$

$$T_t + g(T) = \frac{k\omega T}{p} + \dot{Q} + F_3$$

$$q_t + g(q) = S + F_4$$

$$\psi_p = \frac{RT}{p}$$

$$\omega_p + \frac{1}{a\cos\phi}(v\cos\phi)_\phi + \frac{1}{a\cos\phi}u_\lambda = 0 \quad (1)$$

where,

$$g(X) = \frac{1}{a\cos\phi}(Xu)_\lambda + \frac{1}{a\cos\phi}(Xv\cos\phi)_\lambda + (X\omega)_p$$

In (1), λ, ϕ and p represent the three independent variables of longitude, latitude and pressure. F_i represents vertical and subgrid-scale processes, $\dot{Q}$, the non-adiabatic heating effects and S, the source and sink of moisture.

We now divide longitude into a total of K domains which have common boundaries at the meridians $\lambda_1, \lambda_2, \ldots \lambda_k, \lambda_1$. as indicated in Fig. 1. Further, we defiine $\overline{X_k}$ as the mean value of some quantity X in the kth domain and X_k' as the deviation from $\overline{X_k}$. Such a breakdown of the longitude structure of variable X suggests the following integral relationships :

$$X(\lambda, \phi, p, t) = \overline{X_k}(\phi, p, t) + X_k'(\lambda, \phi, p, t),$$

$$\int_{\lambda_{k-1}}^{\lambda_k} X\,\partial\lambda = \overline{X_k}(\lambda_k - \lambda_{k-1}),$$

$$\int_{\lambda_{k-1}}^{\lambda_k} X'\,\partial\lambda = 0$$

and

$$\int_{\lambda_{k-1}}^{\lambda_k} \frac{\partial X}{\partial\lambda}\,\partial\lambda = \overline{X}(\lambda_k) - X(\lambda_{k-1}) \quad (2)$$

In terms of the notation adopted in (2), we can define the total zonal average of quantity X as;

$$\langle X \rangle = \frac{1}{2\pi}\sum_{k=1,K}(\lambda_k - \lambda_{k-1})\overline{X_k} \quad (3)$$

The relationships shown in (2) and (3) illustrate the concept of domain averaging in longitude. If $K = 1$, the problem reduces to the conventional zonally averaged or zonally symmetric model (Hunt 1973) with $X(\lambda_k) = X(\lambda_{k-1})$. In that special asec zonal derivatives vanish.

In the general case of K domains, such derivatives reduce to the differences of the perturbation quantities evaluated at the longitudinal boundaries of each domain. Even though the individual deviations summed in longitude between 0 and 2π must vanish, a point which allows an integral constraint on the calculation of the deviations, each derivative provides information regarding the interaction of each domain with its neighbours. Such terms act as physical links between adjacent domains.

With the integral relationships defined in (2), the basic equation set (1) may be rewritten to represent the basic state of the kth domain. The basic set becomes :

$$\bar{u}_t = f\bar{v} - \overline{M}(\bar{u}) + \overline{D}(u') + \overline{I}(\lambda) + \overline{F_1}$$

$$\bar{v}_t = -f\bar{u} - \overline{M}(\bar{v}) + \overline{D}(v') + \overline{I}(\phi) + \overline{F_2} + \frac{1}{a}\bar{\psi}_\phi$$

$$\overline{T}_t = -\overline{M}(\overline{T}) + \overline{D}(T') + \overline{I}(T) + \overline{F_3} + \dot{Q}$$

$$\overline{q}_t = -\overline{M}(\bar{q}) + \overline{D}(q') + \overline{I}(q) + \overline{F_4} + S$$

$$\overline{\omega}_p + \frac{1}{a\cos\phi}(\bar{v}\cos\phi)_\phi = \overline{I}(m)$$

$$\bar{\psi}_p = -\frac{R\overline{T}}{p} \quad (4)$$

The subscript denoting the kth domain introduced in (2) will be subsequently assumed.

In the above set $\overline{M}(\overline{X})$ represents the meridional and vertical flux of $\overline{X}$ by the mean motions of the kth domain. For example, $\overline{M}(\bar{u})$ is defined as:

$$\overline{M}(\bar{u}) = \frac{1}{a\cos\phi}(\bar{u}\bar{v}\cos\phi)_\phi + (\bar{u}\,\bar{\omega})_p - \frac{1}{a}\bar{u}\,\bar{v}\tan\phi \quad (5)$$

$\overline{D}(x')$ represents the meridional and vertical fluxes by deviations from the mean quantities in the kth domain, for example .

$$\overline{D}(u') = \frac{-1}{a\cos\phi}\overline{(u'v')}\cos\phi)_\phi - \overline{(u'\omega')}_p + \frac{1}{a}\overline{u'v'}\tan\phi \quad (6)$$

The zonal fluxes and inter-domain interaction terms are represented by $\overline{I}$ which are defined by :

$$\overline{I}(\lambda) = \frac{-1}{a\cos\phi}[u(\lambda_k)^2 - u(\lambda_{k-1})^2]\,d_k + \frac{1}{a\cos\phi}[\psi(\lambda_k) - \psi(\lambda_{k-1})] \quad (7)$$

where,

$$d_k = (\lambda_k - \lambda_{k-1})^{-1}.$$

The $\bar{I}$ terms originate from the zonal derivatives in the various equations and represent differences of *point* quantities evaluated at the boundaries of the various domains. As such quantities are not carried as prognostic variables in the model, they must be related to the mean variables of each domain by some closure scheme. Such a scheme, based upon long wave theory is developed by Webster and Lau (1976) and relates properties of the total mean structure of all the domains to a wave structure which defines a field from which the point quantities can be obtained.

Interdomain fluxes of heat and momentum were found by Webster and Lau (1976) and Lau and Webster (1977) to act as strong secondary determiners of the mean structure of the atmosphere. Generally, the interdomain fluxes and interaction terms are significant and are usually about a factor of two or so smaller than the north-south eddy fluxes. For example, in the northern hemisphere summer the heat convergence from the land area into the ocean area near 30°N is equivalent to a heating rate of about 1·5° to 2°K day^{-1}. Consequently, each domain is a strong function of its neighbour(*s*) and the time-scales of one part of the system (*e.g.*, the ocean domain) will be imprinted upon the character of the other parts of the system, and *vice versa*, *via* the interdomain terms.

The $\bar{D}(X')$, terms also require parameterization principally because the X' terms are not forecast. For closure we follow Stone (1974), Green (1970), and Wiin-Nielson and Sela (1971). The common assumption of all these parameterizations is that they depend upon linear baroclinic instability theory and therefore do not properly model transports by mature disturbances. A critical discussion of the various parameterizations is presented by Webster and Lau (1976).

With the various parameterizations the primitive equation atmospheric model is specialized to two levels. The specialization is outlined in Fig. 3. The momentum and heat equations are written at the 250 and 750 mb levels and the continuity equation at the interface of the two layers (500 mb). The lowest layer surmounts a constant flux boundary layer. Over land, the surface temperature is calculated *via* a heat budget method, the full details of which, along with a description of the various heating and dissipative processes, are presented by Webster and Lau (1976). The determination of the ocean surface temperature ($\bar{T}_s$), on the other hand, is a function of both atmospheric and oceanic dynamics and thermodynamics. Its determination will be discussed in the next section.

(b) *The ocean*

The development of an ocean model which is compatible with the simple atmospheric structure shown in Fig. 2 presents a considerable challange. Here we choose an advective version of the Kraus-Turner (1967) model developed by Lau (1976) and used by Webster and Lau (1970) and Lau and Webster (1977). The model provides a fairly good representation of the surface temperature, mixed layer depth and north-south heat transfer. Basic properties are detailed by Lau (1976) and discussed further by Webster and Lau (1976). In this paper we will only present a schematic description of the formulation.

The advective mixed layer model is schematically described in Fig. 4. The upper part of the ocean consists of a well-mixed layer of variable depth $\bar{h}$ of temperature $\bar{T}_s$. The lower part of the ocean is separated from the upper by an abrupt density change which is represented by a heavy dashed line. The large scale circulation in the upper and lower layers and between the layers are represented by heavy arrows. The heat and mechanical energy inputs are shown on the surface of the ocean. Stippling indicates regions where there exist no density discontinuity between the mixed layer and the lower ocean. In such regions convective adjustment modifies the oceanic column during cooling. The ice regime is indicated at the north and south poles. In the truncated ocean (02 in Fig. 2), the ocean domain extends only to 18°N.

The governing equations for $\bar{T}_s$, $\bar{h}$ and $\overline{T_{-h}}$ are given by:

$$(\bar{T}_s)_t + \bar{V}_s \cdot \Delta T_s + \Gamma \overline{w_{-h}} = \frac{2}{h^2}[-(G^* - D^* - \overline{w^*_{-h}} K^*) + \bar{J}(-h)] \quad (8)$$

$$\Delta(\bar{h}_t + \bar{\mathbf{V}}_s \cdot \Delta\bar{h} + \overline{w_{-h}}) = 2[(G^* - D^*) + I(-h) - 2\bar{J}(-h)] \times [\bar{h}(\bar{T}_s - \overline{T_{-h}}) + 2K^*], \quad (9)$$

$$(\overline{T_{-h}})_t + \bar{\mathbf{V}} \cdot \Delta\overline{T} + \overline{w^*_{-h}}\Gamma = R_{s-h}, \quad (10)$$

and $\overline{w^*_{-h}} = \bar{h}_t + \bar{\mathbf{V}}_s + \overline{w_{-h}}$

where $\bar{\mathbf{V}}$ is the large scale circulation velocity vector, Γ is the temperature lapse rate below the mixed layer, $\bar{\mathbf{V}}_s$ is the horizontal velocity vector of the

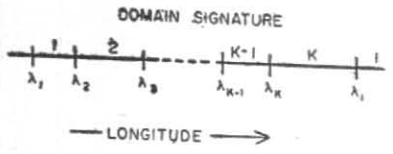

Fig. 1

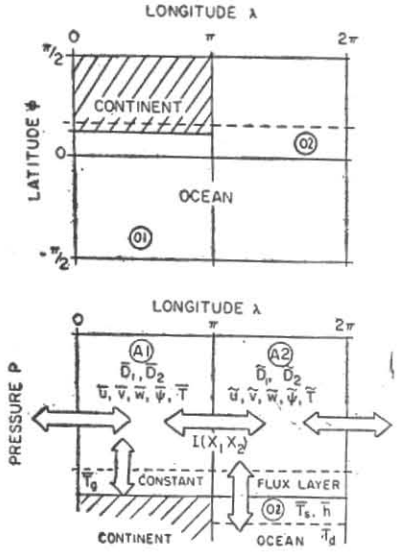

Fig. 2

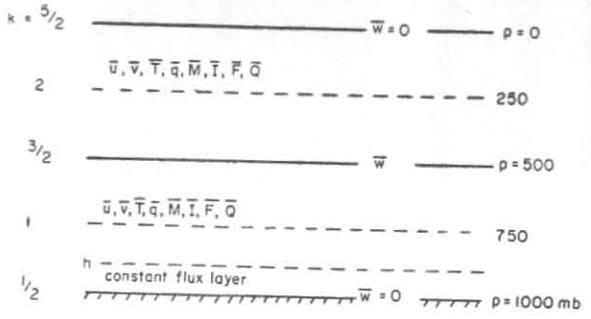

Fig. 3

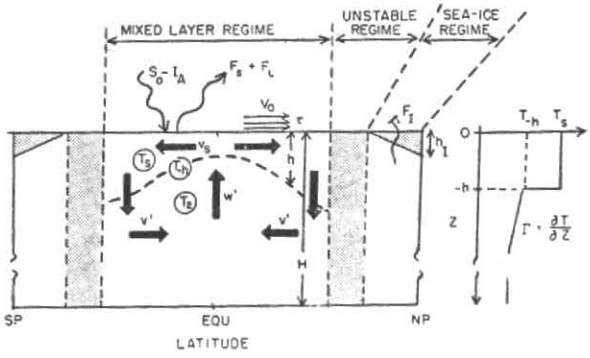

Fig. 4

large scale thermohaline circulation and $\overline{w}_{-h}$ is the associated vertical velocity component evaluated at $z=-h$. G^* and D^* represent the energy input by the wind stress τ and the dissipation within the mixed layer. K^* is a term representing the kinetic energy within the layer ($\alpha \overline{\mathbf{V}}_s \cdot \overline{\mathbf{V}}_s$). R is the incident solar radiation and $I(z)$ is net energy gain by the layer given by :

$$I(z) = R(0) - R(-z) - F^*$$

where F^* is the total upward flux of latent and sensible heat at the surface. $\bar{J}(z)$ represents the integral of $I(z)$ between -z and the surface. $\overline{w}_{-h}^*$ represents the total vertical velocity through the interface at z=-h and is made up by contributions from the large-scale circulation and the wind induced turbulent eddy flux. $\triangle$ is the Heaviside function which modified the structure of (9) depending upon whether there is entrainment of cold deep water or not.

i.e.,

$$\triangle = \begin{cases} 0, \text{ if } \overline{w}^*_{-h} < 0 \text{ ; no entrainment.} \\ 1, \text{ if } \overline{w}^*_{-h} \geqslant 0 \text{ ; entrainment at } z = -h. \end{cases}$$

Details of the derivation and definitions of the various stress, dissipative and energy balance terms may be found in Lau (1976).

Closure of the ocean model requires expressions for the horizontal and vertical velocity components $\overline{\mathbf{V}}_a$ and $\overline{w}_{-h}^*$. It is assumed that the large scale circulation is a result of the density differences existing in the ocean between middle and higher latitudes. Assuming that the mixed layer depth is much less than the depth of the ocean and neglecting salinity effects, the resulting thermal driving force may be written as

$$-\frac{1}{\rho_2 H_a}\frac{\partial \bar{p}}{\partial \phi} = (\overline{T}_1 - \overline{T}_2)\frac{\alpha g}{a}\frac{\partial \bar{h}}{\partial \rho} + \frac{g\bar{h}\alpha}{a}\frac{\partial}{\partial \phi}(\overline{T}_1 - \overline{T}_2)$$

which produces a perturbation meridional current in the lower layer

$$\overline{V'} = A\left[\frac{ag}{a}\frac{\partial}{\partial\phi}\left\{\bar{h}\,(\bar{T}_s - \bar{T}_2)\right\}\right] \qquad (11)$$

A is a free parameter which requires allocation of an arbitrary time scale to (11). We choose $A=5\times10^4$ sec which allows upwelling of the order of 1 to 5 cm day^{-1} which matches open ocean observations of Wyrtki (1961).

Continuity requires that

$$\overline{w_{-h}}^* = -\frac{H}{a\cos\phi}(\overline{V'}\cos\phi)_\phi \qquad (12)$$

which, if we assume the fluid to be non-divergent allows us to calculate the mixed layer meridional velocity component. This is :

$$\overline{V}_s = -\frac{\rho_2}{\rho_s}\frac{H-\bar{h}}{\bar{h}}\overline{V'} \qquad (13)$$

(11)-(13) determine the large scale motion field in terms of the variables $\bar{T}_s$, $\overline{T_{-h}}$ and $\overline{w_{-h}}^*$. Together with (8)-(10) they provide a closed set given only the heat balance at the surface and the atmospheric wind stress.

It should be noted that in the above formulation wind induced upwelling is not included: wind stress in this model acts principally to mix at the thermocline. Work is presently underway to include a wind driven circulation which will allow a further refinement of the model. However, even without this mechanism, it appears that many of the important oceanic processes are included within the model.

3. The Experiment

In this section, the response of the extremely simple model configuration, shown in Fig. 2, to an imposed annual solar heating variation, is discussed. Domains A1 and A2 are described by the two-level primitive equation formulation discussed in the last section. As a first approximation, moist processes are *omitted* from the experiment. A complete hydrology system including a cloud-albedo feedback parameterization will be described in a similar but simpler experiment (Webster and Chou 1977). The ocean domains 01 and 02 use the advective mixed layer formulation.

The annual cycle of the solar heating is given by :

$$S_0 = (1-\alpha)\,S\left(\frac{\pi}{2}\sin\phi\sin\delta + \cos\phi\cos\delta\right) \qquad (14)$$

Where α is the albedo, ϕ is the latitude, δ is the time dependent solar-declination angle and S is the solar constant. To provide a set of initial conditions from which an annual cycle could evolve, the declination angle was set equal to zero (equinox condition). When a statistical equilibrium situation was approached, δ was allowed to become vary and follow an annual cycle.

(a) *The fields*

Figs. 5-12 show the latitude-time plots of the first year of the experiment for the u, v, ω and T fields. The response of each domain (A1 and A2) is shown separately. In all figures the ordinate scale corresponds to latitude and the abscissa to time. On the lower abscissa time is marked off at monthly intervals while on the upper abscissa seasonal markers are denoted.

Fig. 5 shows the zonal velocity component distribution for the A1 domain (*i.e.*, atmosphere above the truncated continent and the ocean to the south) at both the 750 mb and 250 mb levels. Fig. 6 follows an identical format except for domain A2. In the upper troposphere a strong easterly maxima (~ -25 ms^{-1}) forms just equatorward of the continental southern boundary, reaching maximum intensity some four weeks after the summer solstice. The easterly maximum decays rapidly near the autumnal equinox and is replaced by a strong westerly maximum which is centred near 30°N. In the southern hemisphere, which is assumed to be completely oceanic, the predominant features are the strong mid-latitude and sub-tropical westerlies. Near the winter solstice only very light easterlies form near the equator which are accompanied by a weak westerly field further poleward. In the lower troposphere over the northern hemisphere continent rapid changes occur between the seasons. Below the upper level easterlies relatively strong westerlies are evident, which coupled with the meridional velocity component at 750 mb (*see* Fig. 7 for the 250 mb field); provide a strong southwesterly flow. Near the winter solstice strong easterlies couple with the meridional field to give a northeasterly flow. In the southern hemisphere weak easterlies prevail over the low-latitudes with moderate westerlies to the south. It should be

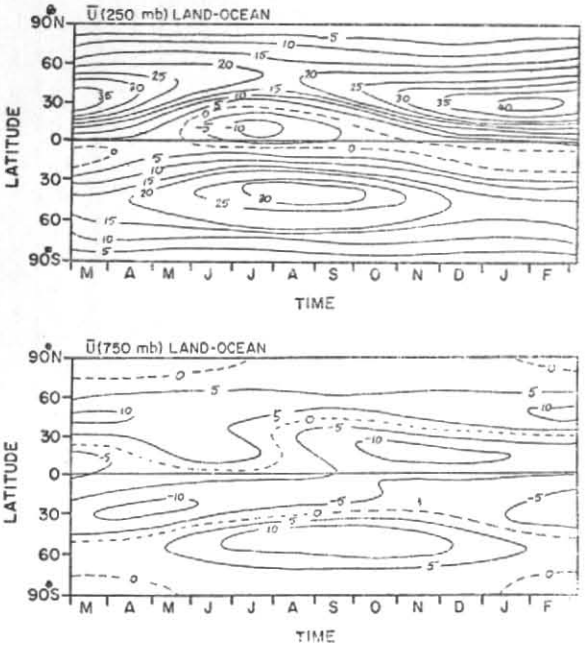

Fig. 5

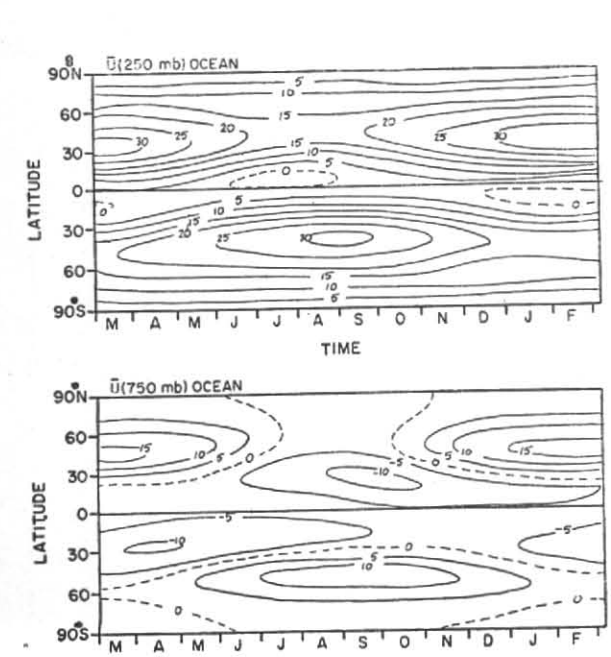

Fig. 6

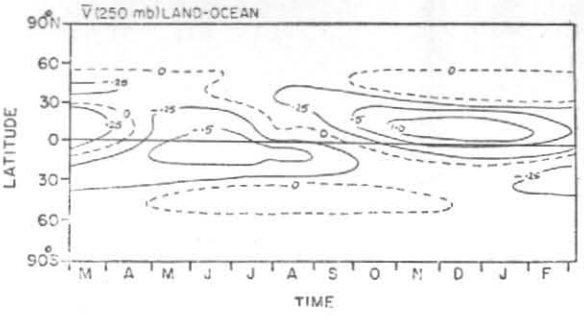

Fig. 7

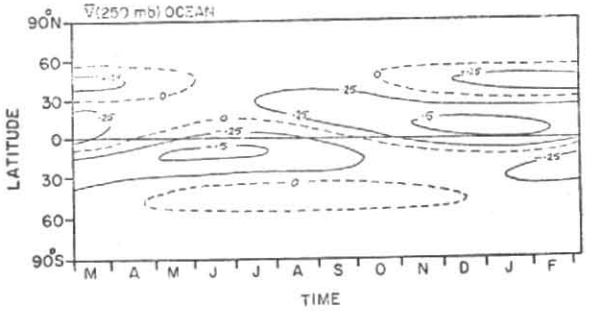

Fig. 8

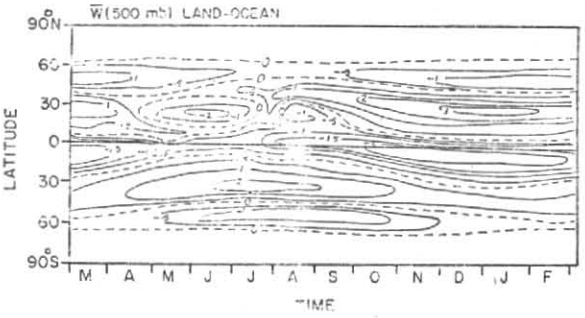

Fig. 9

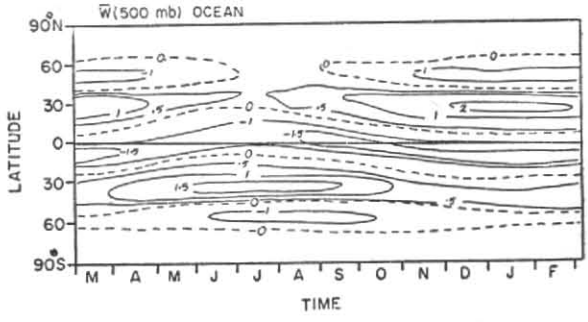

Fig. 10

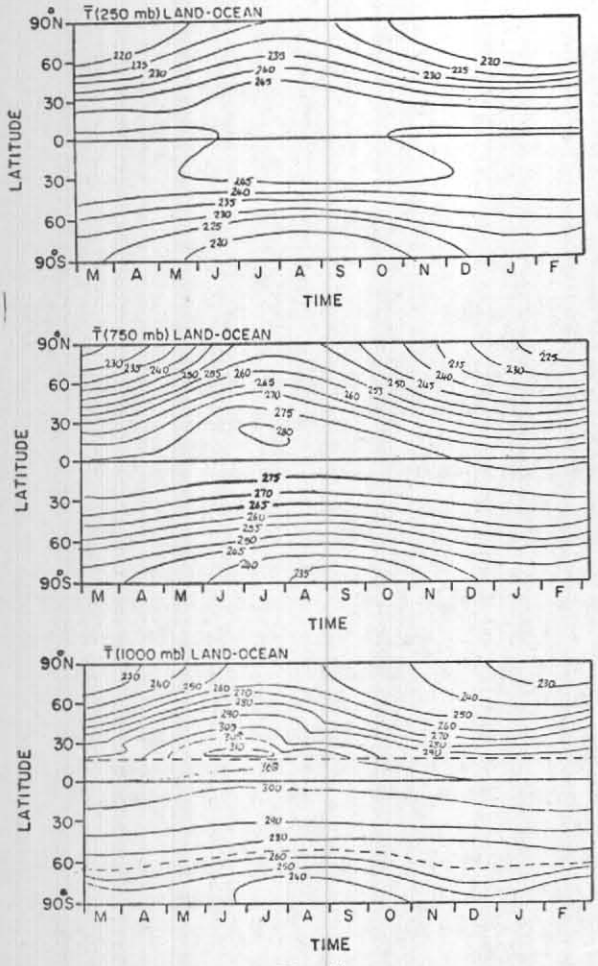

Fig. 11

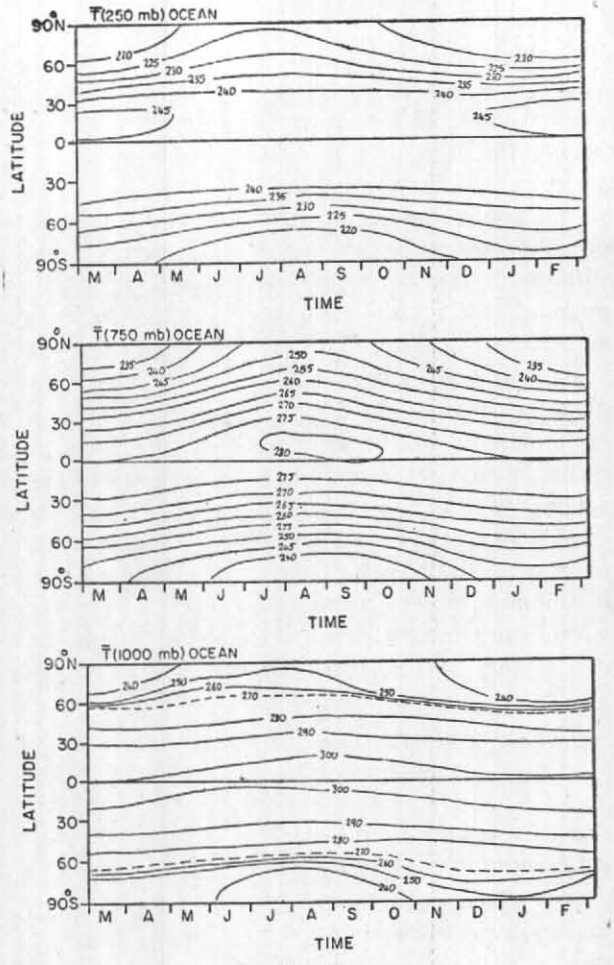

Fig. 12

noted that phase differences occur in both latitude and time between the various maxima at the different levels. This suggests a combination of differing influence which may be attributed to interhemisphere interaction, intersystem interaction (*i.e.*, ocean-atmosphere) and interdomain interaction. Phase differences and the physical relationships, they imply, will be discussed in the next section.

Figs. 7 and 8 show the meridional velocity fields at 250 mb for domains A1 and A2, respectively. The corresponding vertical velocity fields are shown in Figs. 9 and 10. The most significant feature of both $\overline{V}$ distributions is the dominant Hadley-type cell which allows strong southward flow across the equator in summer and a somewhat weaker northward flow in winter. Domain A1 is distinguished by possessing considerably larger magnitudes than its oceanic counterpart, a feature which is also apparent in the vertical velocity structure, and also by possessing maxima more poleward. Phase differences are also observed but it is sufficient to note that the equinoctial transitions are considerably more abrupt at low latitudes adjacent to the continent than over the oceans. This may be seen in both the meridional and vertical velocity components.

A significant feature of the vertical velocity fields is the reversal occurring in late July and August. This 2-3 week reversal, which is also noted in the temperature fields, will be shown to be produced by a combination of ocean and continental effects.

The temperature structure at 1000 mb, 750 mb and 250 mb in domain A1 is shown in Fig. 11 and for domain A2 in Fig. 12. In Figs. 11(a) and 12(a) the temperature in the ocean areas refers to the sea-surface temperature and not the atmospheric temperature. The sea-surface temperature is

determined by the advective mixed-layer model discussed in section 2b. Considering just the surface temperature in domain A1, we note that the field is discontinuous at the sea-land boundary (dashed line). Maximum temperatures occur some weeks after the summer solstice and near 30°N. At this time in the southern hemisphere the ocean is still cooling indicating the longer thermal lag of the ocean. It should be mentioned that without the adjacent interactive ocean, the maximum temperature over land would be reached earlier than shown in Fig. 11(a). What occurs in Fig. 11(a) is a response of the *total* ocean-atmosphere system. As the winter approaches, extremely rapid cooling of the land areas occur which is accompanied by a similar although less-marked cooling of the equatorial oceans of the south. The effect of this is to remove the oceanic maximum temperature, which was north of the equator in summer, to the south of the equator. Note the strong substructure in the surfce temperature field in late July and August. Similar variability was also evident in the ω and v fields.

The surface temperature structure of domain A2 (Fig. 12a) shows a somewhat smaller variation with time compared to that in A1. The southern ocean is essentially the same as that in domain A1 except for small phase and amplitude variations.

The temperature variations in the upper troposphere can be seen from Figs. 11(b) and (c) and 12(b) and (c) to bear resemblence to the character of the surface variations, especially in domain A1. The 750 mb and 250 mb temperature fields for A1 and A2 are quitesimilar and possess only small phase differences.

The 750 mb temperature fields of A1 and A2 are quite similar over the southern oceans except for quite small amplitude and phase differences noted earlier with the respective surface temperatures. This is also true for the 250 mb fields. The maximum occurring on either side of the equator in the northern hemisphere summer in A1 has been noted by Newell *et al.* (1972). It is interesting to note that evidence of a strong annual cycle in the northern hemisphere portion of A2 occurs more at 750 mb and 250 mb than at the surface. The reason for this is probably that the interdomain fluxes are more effective in changing atmospheric structure than the ocean which possesses a larger self-inertia. However, as the occurrence of the mid-latitude temperature maximum at 750 mb is somewhere between the ocean surface temperature maximum and the adjacent continental surface temperature, it appears that the tropospheric temperature structure over the ocean feels the influence in both oceanic and continental regions. Similarly, as the 750 mb temperature over the land in A1 occurs after the surface maximum but *before* the adjacent 750 mb temperature in A2, it is obvious that the continental atmosphere feels the influence of the adjacent domain also.

(b) *Phase variations*

In discussing the amplitude variations, we noted certain fields approached maximum and minimum values at different times. To study these differences we consider the variations of $\bar{u}$, $\bar{v}$, $\bar{T}$ and $\bar{\omega}$ for various latitudes in domains A1 and A2. The distributions at the three latitudes are shown in Figs. 13, 14, 15 and 16 respectively. In all diagrams the vertical lines denote seasonal markers relative to the upper abscissa upon which the northern hemisphere seasons are depicted.

The zonal velocity component at 26°N is shown in Fig. 13. At 250 mb the easterly jet stream attains a maximum some time after the summer solstice and slightly ahead with the minimum 250 mb westerly at 18°N in the adjacent ocean domain. During winter the upper westerlies over the land attain maximum values a few weeks ahead of the corresponding A2 component. The meridional component (Fig. 14) suggests a much stronger Hadley-type cell than that which occurs over the ocean and is also nearly in phase with the solar heating.

The 18°N distributions suggest extremely large longitudinal differences in the simulated annual cycle. The important point which we reiterate here is that the distributions in A1 and A2 possess character which may not be explained *solely* in terms of the underlying boundary condition but rather as a complicated composite of influences. It would appear that the atmospheric structure over the land areas is influenced a great deal by the adjacent ocean regions to the south *and* also to the east; the latter influence occurring *via* the longitudinal interaction terms discussed in section 2. That such longitudinal influence exists is not a revelation as the basic process was explained by Smagorinsky (1953). However that such a simple model as the one used in this study is able to isolate some of the longitudinal influence is heartening and suggestive of further work.

The field reversals occurring near day 150 are most evident in Figs. 14 and 15. The maximum values of v and ω correspond to the maximum

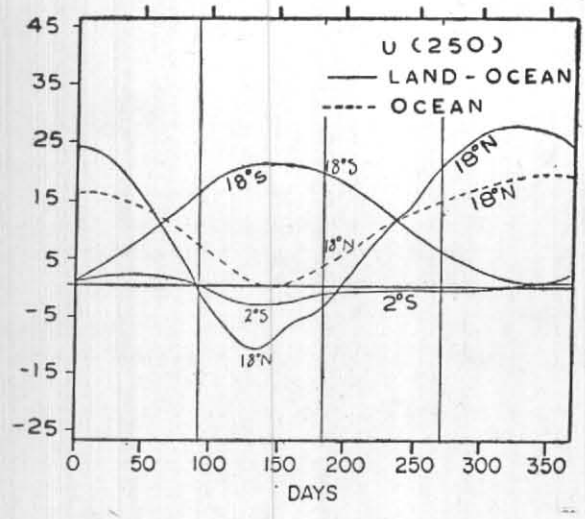

Fig. 13

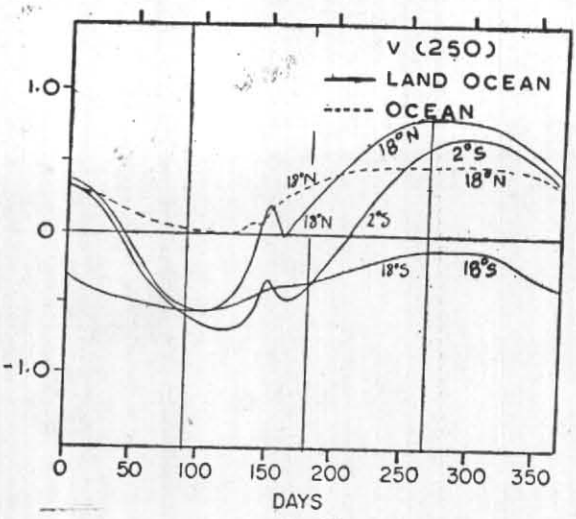

Fig. 14

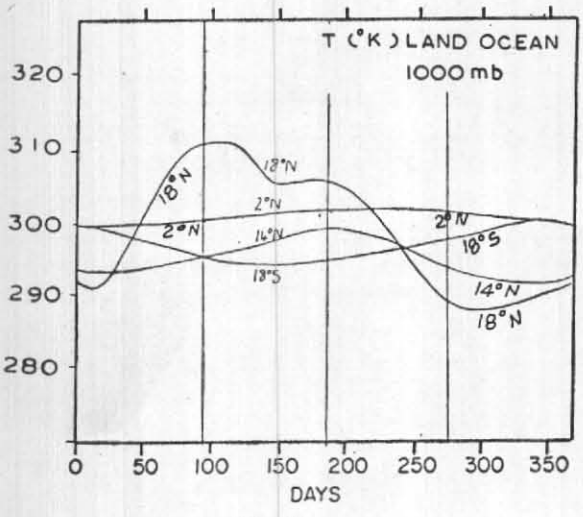

Fig. 15

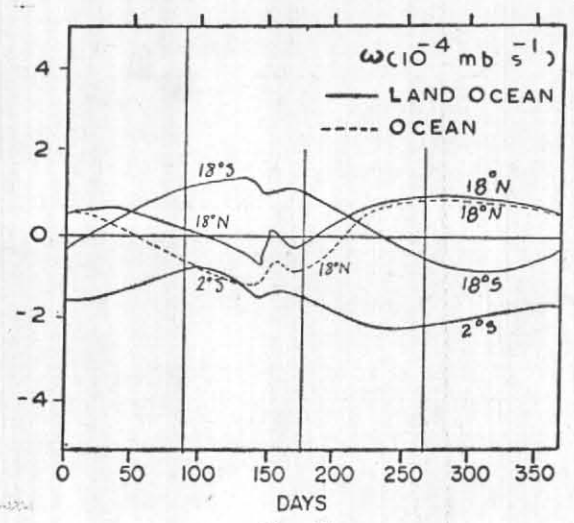

Fig. 16

sensible heating by the land. As the sun retreats southward, the v-field at 18°N approaches zero and ω actually reverses. However the ocean has yet to reach a maximum and when this occurs both v and ω (also T in Fig. 15) reassume their early summer distributions.

The character of the near equatorial fields (2°S) and difference between the two domains varies from that appearing in Fig. 13. In Fig. 14(a) the zonal velocity components are considerably smaller than those further north at all times of the year. In domain A1 weak easterlies (<10 ms^{-1}) prevail in the lower troposphere and are surmounted at 250 mb by stronger easterlies in summer whose peak value occurs even later than that of the easterly maximum further to the north. Over the adjacent ocean moderate westerlies are apparent at 250 mb with a maximum occurring near the winter solstice. The meridional velocity field shown in Fig. 14(b) shows a similar character to the fields at 26°N. Both domains possess relative strong Hadley-type circulations and both possess strong southerly flow at 250 mb in the northern hemisphere summer which is stronger than the winter-time return flow. It is interesting to note that the maximum northward flow in A1 occurs before the winter solstice although in phase with the $\bar{v}$ structure to the north. The temperature fields (Fig. 14c) show much less variability than their northern counterparts. At the surface the A2 temperature structure shows a

continual warming which, as mentioned before, is a consequence of the first year of integration. Longer integrations will allow the ocean to come into "equilibrium" with the atmosphere at low latitudes (*see* Lau 1976 and Wesbter and Lau 1976).

In the southern "oceans" the differences between the two domains has lessened but each still retains an independent character which would seem to be influenced by the differing structure of the northern part of each domain. Fig. 15(a) shows strong westerlies dominating the southern hemisphere winter upper troposphere. The maximum in A1 occurs some weeks ahead of the slightly more intense maximum in A2. The A1 maximum occurs at roughly the same time as the easterly maximum at 26°N (*see* Figs. 5b and 13a). The $\bar{v}$ fields (Fig. 15b) show weak southerly flow over most of the year with each domain possessing almost the same amplitudes and similar phases. The temperature fields show a strong annual cycle with only slight differences in magnitudes. At the surface the temperature at A2 is cooler which probably corresponds to the stronger mixing by the more intense winds shown in Fig. 15(a).

4. Concluding Remarks

The response of an extremely simple ocean-atmosphere interaction model to an imposed solar heating cycle has been presented. Comparisons of the fields from various domains at different latitudes and times signify the importance of the treatment of the total system (*i.e.*, atmosphere and ocean) in order to obtain correct phasing and location of the atmosphere and ocean response.

The structure of the model used in this study is the simplest prototype of the domain averaged model formulation which allows at least in indication of the interactions between the atmospheres and oceans on the annual time sacle. However to approach a better understanding of even the macroscale monsoon processes, the following improvements to the formulation and structure will be implemented :

(*i*) Extend the integration to allow for a number of annual cycles. The main reason for this is to allow the atmosphere and the advective-mixed layer model to come into a common state of equilibrium.

(*ii*) Include moist processes and cloud-feedback parameterizations. Such processes are included in Webster and Chou (1977) for a simpler experiment. Neglect was not intended to belie the importance of moist processs. On the contrary, such processes are probably of great importance and allow the entrance of further time scales into the monsoon sequence. Our omission stems from wanting to develop the model piecemeal and in this manner establish a control study with each added sophistication. We feel that by this process we enlarge the possibility of being able to diagnose as what still constitutes a complicated model.

(*iii*) Increase the number of domains. The domain-averaged formulation discussed in sections 1 and 2 allows for the addition of many domains of arbitrary latitudinal extent but with the constraint of possessing constant longitudinal extent. The longitudinal extent of each domain is, however, quite arbitrary. It is felt that the number of domains needed to be able to anticipate nuances of the gross state of the monsoon would be five atmospheres and five oceans, where the continent is divided into at least three parts with the western part extending southward across the equator in order to model the Afro-Asian complex (Webster and Lau 1976).

(*iv*) The inclusion of orographic features such as the Himalayan Massif and

(*v*) The consideration of the wind driven oceanic transport. In suggesting a minimum of five oceans in (*iii*) above, it is anticipated that each ocean basin be divided into an eastern part and a western part. In this manner an oceanic east-west temperature gradient may be induced by atmospheric wind stress. Oceanic transports would be produced by both "thermo-haline" and wind driven processes.

In this paper we purposely have not compared the response of the model with real atmospheric observations except for gross climatological features and phase dependencies. This is because the simplicity of the domain structure chosen for the study renders comparison inappropriate. However, the fields that are produced in the various domains are interesting and indicative of a some-

what realistic annual cycle. Most importantly, they give some confidence that the additions outlined in (*i*) to (*v*) above will produce results which will allow a meaningful comparison with observations.

Acknowledgement

This work was supported by the Atmospheric Sciences Section, National Science Foundation, Grant DES-74-01702.

REFERENCES

Bryan, K., Manabe, S. and Paconowski, R.C.	1975	*J. Phys. Ocean.*, **5**, pp. 30-46.
Green, J. S. A.	1970	*Quart. J.R. Met. Soc.*, **96**, pp. 157-185.
Hahn, D. G. and Manabe, S.	1975	*J. atmos. Sci.*, **32**, pp. 1515-1541.
Hunt, B. G.	1973	*Tellus*, **15**, pp. 337-354.
Kraus, E. B. and Turner, J. A.	1967	*Ibid.*, **19**, pp, 98-105.
Lau, K.M.W.	1976	A simple advective global mixed-layer model (submitted to *J. Phys. Ocean*).
Lau, K.M.W. and Webster, P.J.	1977	Simulation of the annual cycle with a simple ocean-atmosphere interaction model (to be submitted to *J. atmos. Sci.*)
Manabe, S., Bryan, K. and Spelmen, M.J.	1975	*J. Phys. Ocean.*, **5**, pp. 3-29.
Newell, R. E., Kidson, J. W., Vincent, D. G. and Boer, G. J.	1972	*The General Circulation of the Tropical Atmosphere and Interactions with Extra-tropical Latitudes* ,**1**, MIT Press, Mass, Inst. of Tech, Cambridge, ME, 258 pp.
Ramage, C. S.	1971	*Monsoon Meteorology*, International Geophysical Series **15**, Academic Press, 296 pp.
Ramage, C. S., and Raman, C. R. V.	1972	*Meteorological Atlos of the International Indian Ocean Expedition*, **2**, National Sci., Foundation, Wash. D.C., 121 Charts.
Sadler, J.	1969	Mean circulation and cloudiness during the development of the southwest monsoon over India and Southeast Asia, *Proc. Conf. Summer Monsoon of Southeast Asia*, (C.S. Ramage, Ed.,) Naval Weather Res. Facility, Norfolk, VA, p 13-28 (NTIS No AD-876-667).
	1975	'The upper tropospheric circulation of the global tropics', UHMET 75-05 Dep. Met., Univ. Hawaii, 35 pp..
Sadler, J. and Harris, B. E.	1970	'The mean tropospheric circulation over Southeast Asia and its neighbouring areas' AFCRL-70-0489 and HIG-70-26, Hawaii Int. of Geophys, Univ. Hawaii, 38 pp. (NTIS No AD-715912).
Shukla, J.	1975	*J. atmos. Sci.*, **32**, pp. 503-511.
Smagorinsky, J.	1953	*Quart. J.R. Met. Soc.*, **97**, pp. 342-366.
Stone, P. H.	1974	*J. atmos. Sci.*, **31**, pp. 444-456.
Washington, W. and Daggapaty, S. M.	1975	*Mon. Weath. Rev.*, **103**, pp. 105-114.
Webster, P. J. and Lau, K. M. W.	1977	'A simple ocean-atmosphere climate model : Basic model and a simple experiment' (to appear in *J. atmos. Sci.*, July 77).

REFERENCES (Contd.)

Webster, P. J. and Chou, L. 1977 Variations in the monsoon sequence (to appear in *J. atmos. Sci.*).

Wiin. Nielson, A. and Sela, J. 1971 *Mon. Weath. Rev.*, **99**, pp. 447-459.

Wyrtki, K. 1961 *Deep Sea Res.*, **8**, pp. 39-64.

DISCUSSION

(Paper presented by Peter J. Webster)

JOHN A. YOUNG : Have you done any linear analysis of either transient or stationary 'waves' in the model ?

AUTHOR : Not as yet. However, we realise the importance of such an analysis and intend to perform it in the future.

B.M. MISRA : How are precipitation and vertical velocity related in the model ?

AUTHOR : Only an example of the model with precipitation was shown. However, there are two types of latent heat release in the model convective and large scale. The former depends upon the saturation of the atmosphere and the vertical velocity whereas the second process depends only on moisture saturation.